Report

Current Biology

Tropomyosin Isoforms Specify Functionally Distinct Actin Filament Populations In Vitro

Graphical Abstract

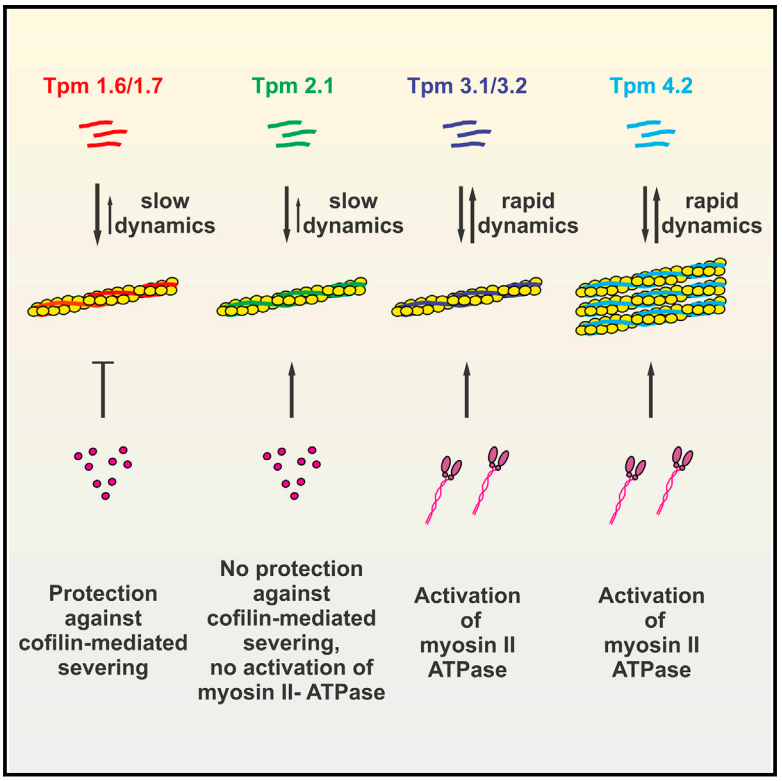

Authors

Gergana Gateva, Elena Kremneva, Theresia Reindl, ..., Dietmar J. Manstein, Alphée Michelot, Pekka Lappalainen

Correspondence

pekka.lappalainen@helsinki.fi

In Brief

Gateva et al. report that distinct tropomyosin isoforms segregate to different actin filaments and can specify functional properties of distinct actin filament populations. They also provide evidence that functions of tropomyosins in myosin II activation and actin filament stabilization correlate with the dynamics of their actin interactions.

Highlights

- Stress-fiber-associated tropomyosin isoforms segregate to different actin filaments
- Tropomyosin isoforms bind F-actin with different dynamics
- Dynamic tropomyosin isoforms activate non-muscle myosin II
- Stable tropomyosin isoforms protect actin filaments from ADF/cofilin

Gateva et al., 2017, Current Biology *27*, 705–713
March 6, 2017
http://dx.doi.org/10.1016/j.cub.2017.01.018

Current Biology
Report

Tropomyosin Isoforms Specify Functionally Distinct Actin Filament Populations In Vitro

Gergana Gateva,[1] Elena Kremneva,[1] Theresia Reindl,[2] Tommi Kotila,[1] Konstantin Kogan,[1] Laurène Gressin,[3] Peter W. Gunning,[4] Dietmar J. Manstein,[2] Alphée Michelot,[5] and Pekka Lappalainen[1,6,*]
[1]Institute of Biotechnology, University of Helsinki, P.O. Box 56, 00014 Helsinki, Finland
[2]Institute for Biophysical Chemistry, Hannover Medical School, 30625 Hannover, Germany
[3]Biosciences and Biotechnology Institute of Grenoble, LPCV/CNRS/CEA/UGA/INRA, 38054 Grenoble, France
[4]Oncology Research Unit, School of Medical Sciences, UNSW Australia, Sydney, NSW 2052, Australia
[5]Aix-Marseille University, CNRS, IBDM, 13284 Marseille, France
[6]Lead Contact
*Correspondence: pekka.lappalainen@helsinki.fi
http://dx.doi.org/10.1016/j.cub.2017.01.018

SUMMARY

Actin filaments assemble into a variety of networks to provide force for diverse cellular processes [1]. Tropomyosins are coiled-coil dimers that form head-to-tail polymers along actin filaments and regulate interactions of other proteins, including actin-depolymerizing factor (ADF)/cofilins and myosins, with actin [2–5]. In mammals, >40 tropomyosin isoforms can be generated through alternative splicing from four *tropomyosin* genes. Different isoforms display non-redundant functions and partially non-overlapping localization patterns, for example within the stress fiber network [6, 7]. Based on cell biological studies, it was thus proposed that tropomyosin isoforms may specify the functional properties of different actin filament populations [2]. To test this hypothesis, we analyzed the properties of actin filaments decorated by stress-fiber-associated tropomyosins (Tpm1.6, Tpm1.7, Tpm2.1, Tpm3.1, Tpm3.2, and Tpm4.2). These proteins bound F-actin with high affinity and competed with α-actinin for actin filament binding. Importantly, total internal reflection fluorescence (TIRF) microscopy of fluorescently tagged proteins revealed that most tropomyosin isoforms cannot co-polymerize with each other on actin filaments. These isoforms also bind actin with different dynamics, which correlate with their effects on actin-binding proteins. The long isoforms Tpm1.6 and Tpm1.7 displayed stable interactions with actin filaments and protected filaments from ADF/cofilin-mediated disassembly, but did not activate non-muscle myosin IIa (NMIIa). In contrast, the short isoforms Tpm3.1, Tpm3.2, and Tpm4.2 displayed rapid dynamics on actin filaments and stimulated the ATPase activity of NMIIa, but did not efficiently protect filaments from ADF/cofilin. Together, these data provide experimental evidence that tropomyosin isoforms segregate to different actin filaments and specify functional properties of distinct actin filament populations.

RESULTS AND DISCUSSION

Actin filaments assemble into diverse three-dimensional arrays to execute a wide variety of processes in eukaryotic cells. These actin filament arrays are characterized by distinct protein compositions and dynamic properties, but the underlying molecular mechanisms are incompletely understood [1, 8]. To elucidate the principles by which functionally distinct actin filament populations can be generated in cells, we focused on analyzing stress-fiber-associated tropomyosin isoforms. Stress fibers are contractile actomyosin bundles that contribute to cell morphogenesis, adhesion, migration, and mechanosensing [9]. Stress fiber assembly depends on several proteins promoting actin filament nucleation and polymerization, and different stress fiber types are decorated by partially non-overlapping sets of actin-binding proteins [7, 10–14]. Six tropomyosin isoforms (Tpm1.6, Tpm1.7, Tpm2.1, Tpm3.1, Tpm3.2, and Tpm4.2) associate with stress fibers in osteosarcoma cells (Figures 1A and 1B; Figure S1A). Importantly, these isoforms display partially different localization patterns along stress fibers and, based on RNAi experiments, are functionally non-redundant [7]. Therefore, they may specify functionally distinct actin filament populations within the stress fiber network. However, whether distinct tropomyosin isoforms indeed segregate to different actin filaments has not been experimentally demonstrated. Moreover, the biochemical properties of actin filaments decorated by different tropomyosin isoforms have not been systematically studied.

To examine the six stress-fiber-associated tropomyosin isoforms, we expressed and purified them as non-tagged versions and as superfolder GFP (sfGFP)- or mCherry-fusion proteins. In all cases, an alanine-serine extension was introduced to mimic amino-terminal acetylation [15]. In the fluorescent fusion proteins, sfGFP/mCherry was linked to the N termini of the tropomyosins because such fusion proteins localize properly to the stress fiber network in cells and can rescue the knockout phenotype (Figure S1B) [7]. Moreover, a recent biochemical study demonstrated that an amino-terminal *S. pombe* tropomyosin fluorescent fusion binds actin filaments and forms similar end-to-end interactions compared to endogenous acetylated tropomyosin

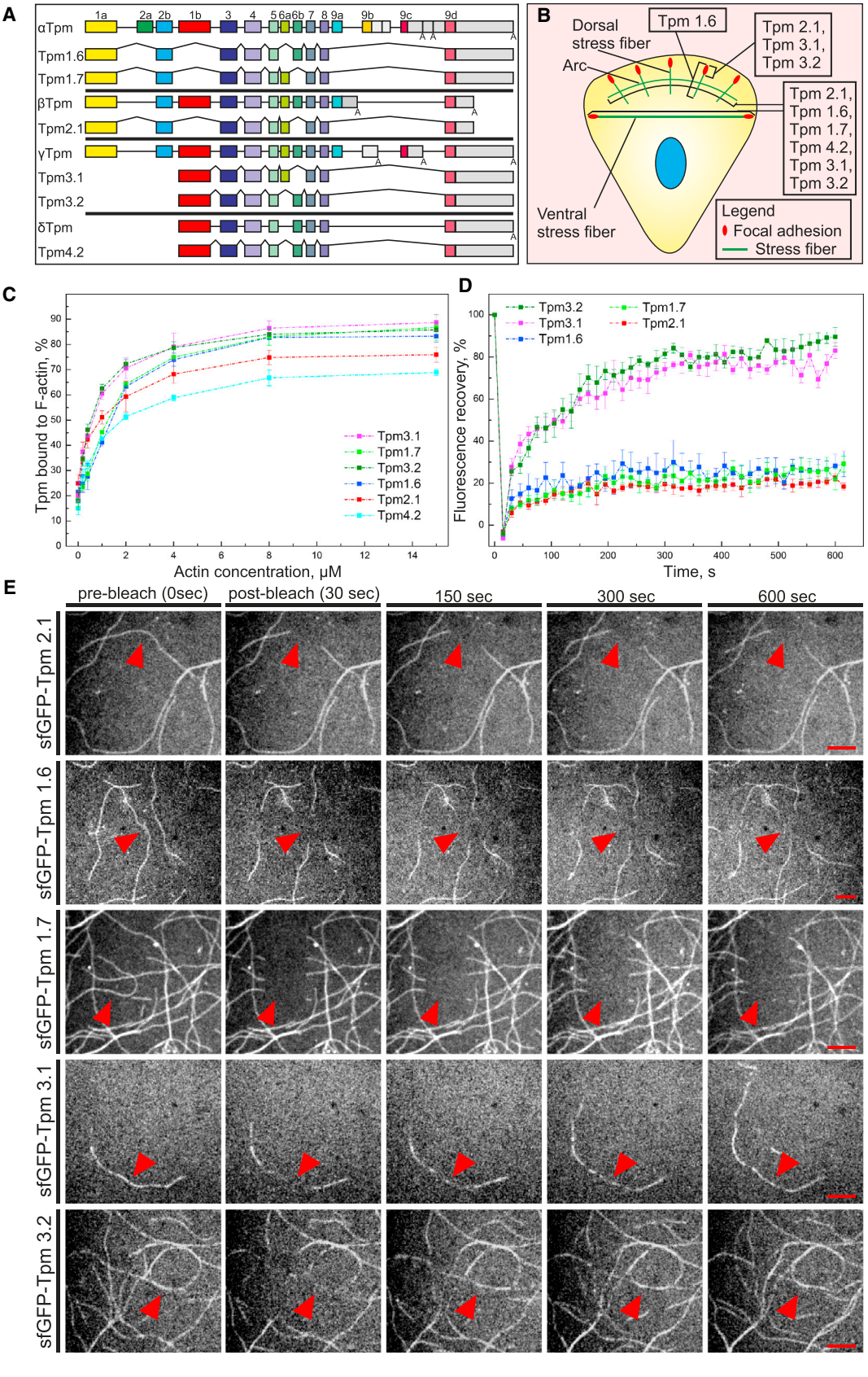

(legend on next page)

[16]. The actin filament co-sedimentation assay was first applied to examine the binding of non-tagged and sfGFP-tagged tropomyosins to non-muscle β/γ-actin filaments. Consistent with earlier work [17], the stress-fiber-associated tropomyosins bound β/γ-actin filaments with high affinity (K_d < 1 μM) and the N-terminal sfGFP fusion did not interfere with F-actin binding (Figure 1C; Figure S1C). This was also supported by in vitro total internal reflection fluorescence (TIRF) microscopy experiments demonstrating that the fluorescent fusions of tropomyosins decorated non-labeled β/γ-actin filaments. However, tropomyosins do not efficiently interact with rhodamine-labeled actin, because tropomyosins and rhodamine-actin segregated on filaments in experiments where only a small fraction (5%) of actin monomers was labeled (Figure S1D). Whereas sfGFP fusions of Tpm1.6, Tpm1.7, Tpm2.1, Tpm3.1, and Tpm3.2 interacted strongly with individual actin filaments in the TIRF microscopy assay, sfGFP-Tpm4.2 bound only to actin filament bundles, induced either by methylcellulose or myosin II, with high affinity (Figures S2A and S2B; data not shown). Mechanistic principles by which Tpm4.2 preferentially interacts with actin filament bundles (at least in our TIRF setup) remain to be elucidated. A simple interpretation is that, unlike the other tropomyosins, Tpm4.2 promotes filament bundling and only interacts strongly with actin filaments that are bundled. This property may be linked to its cellular function in myosin II recruitment to stress fibers [7].

Fluorescence recovery after photobleaching (FRAP) was applied to examine the dynamics of stress-fiber-associated tropomyosins on actin filaments. The assay was first performed on individual actin filaments with Tpm1.6, Tpm1.7, Tpm2.1, Tpm3.1, and Tpm3.2. Interestingly, sfGFP fusions of Tpm1.6, Tpm1.7, and Tpm2.1 displayed only very slow recovery on bleached actin filament segments, whereas the fluorescence recovery of sfGFP fusions of Tpm3.1 and Tpm3.2 on actin filaments was relatively rapid (Figures 1D and 1E). Because Tpm4.2 does not bind individual actin filaments with high affinity, the FRAP assay was also performed on actin filament bundles induced by methylcellulose. To confirm that we indeed measured the dynamics of actin-filament-associated tropomyosins, samples were spiked with 5% rhodamine-labeled actin to visualize the filament bundles. Importantly, sfGFP-Tpm4.2 displayed similar rapid recovery on actin filament bundles compared to sfGFP-Tpm3.1 and sfGFP-Tpm3.2, whereas the fluorescence recoveries of sfGFP-Tpm1.6, sfGFP-Tpm1.7, and sfGFP-Tpm2.1 were very slow, further confirming the differences in the dynamics of actin filament association between these tropomyosins (Figures S2C and S2D). Together, these data reveal that the long stress-fiber-associated tropomyosin isoforms derived from the *Tpm1* and *Tpm2* genes display stable association with actin filaments, whereas the short isoforms derived from the *Tpm3* and *Tpm4* genes display dynamic association with actin filaments. This correlates with the stronger cooperativity of actin binding observed with long tropomyosins compared with short isoforms [17].

We next asked whether the spatial segregation of tropomyosin isoforms is an intrinsic property of the tropomyosin proteins. To test this, we examined whether different tropomyosin isoforms, when incubated in combination with each other and actin filaments, bind to same filaments or whether they segregate into different actin filaments or filament segments. Control experiments performed with sfGFP and mCherry fusions of the same tropomyosin isoform demonstrated that the two proteins with different fluorescent tags do not segregate along actin filaments. This indicates that the N-terminal fluorescent fusions do not alter the ability of tropomyosins to form end-to-end oligomers. Please note that the number of tropomyosin-decorated actin filaments appeared to differ in the case of distinct tropomyosin isoforms. This may arise from differences in the cooperativity of actin filament association between these tropomyosin isoforms. Importantly, when sfGFP and mCherry fusions of different tropomyosin isoforms were co-incubated with actin, the two proteins often segregated into different segments along the actin filaments (Figure 2A; Figure S3). Quantification of co-localization indices of different tropomyosin pairs provided evidence that whereas the tropomyosin isoforms generated from the same gene (Tpm1.6 and Tpm1.7 as well as Tpm3.1 and Tpm3.2) can co-polymerize on actin filaments, the isoforms generated from different *tropomyosin* genes are generally not capable of co-polymerizing on actin filaments and thus form segments along the filaments. The only exception was Tpm2.1, which appeared to be able to co-polymerize with Tpm3.1 and Tpm3.2 but not with Tpm1.6 and Tpm1.7 (Figure 2B). These data provide evidence that different tropomyosin isoforms can segregate into different actin filaments/filament segments and are capable of generating actin filament populations that are decorated by a specific tropomyosin isoform or a specific combination of tropomyosin isoforms.

Do actin filaments decorated by different tropomyosin isoforms display functional differences? We first approached this question by examining the effects of stress-fiber-associated tropomyosins on cofilin, because these two proteins have been shown to compete for F-actin binding both in vitro and in cells [5, 18–20]. The only exception reported so far is Tpm1.2,

Figure 1. Interactions of Different Tropomyosin Isoforms with F-Actin

(A) Schematic representation of the intron-exon structures of the four human *tropomyosin* genes and the six stress-fiber-associated tropomyosin isoforms expressed from these genes (see also Figure S1A).

(B) Distribution of the tropomyosin isoforms within the stress fiber network of U2OS cells.

(C) Binding of non-labeled tropomyosins to β/γ-actin filaments was examined by a co-sedimentation assay. The concentration of the tropomyosin dimers was 0.5 μM, and the concentration of actin was varied from 0.2 to 15 μM. Data are represented as average ± SEM; n = 3 independent experiments. Please note that the lines do not represent curve fitting but serve simply as connectors between the data points.

(D and E) Dynamics of tropomyosin binding to β/γ-actin filaments was examined by fluorescence recovery after photobleaching (FRAP) experiments. For the assay, 0.8 μM sfGFP fusions of tropomyosin isoforms were mixed with pre-polymerized 0.6 μM unlabeled actin. Tropomyosins did not form any visible filament-like structures in the absence of actin, demonstrating that structures seen in the images are tropomyosin-decorated actin filaments. A few frames were recorded prior to bleaching. The fluorescence recovery was followed for 10 min after bleaching by obtaining images every 15 s. Representative examples of the FRAP data are shown in (E), and the averaged recovery curves for all tropomyosin isoforms tested are shown in (D). Data are represented as average ± SEM; n = 5–6 filaments from three independent experiments (see also Figure S2). Red arrowheads indicate bleached filament regions. Scale bars, 10 μm.

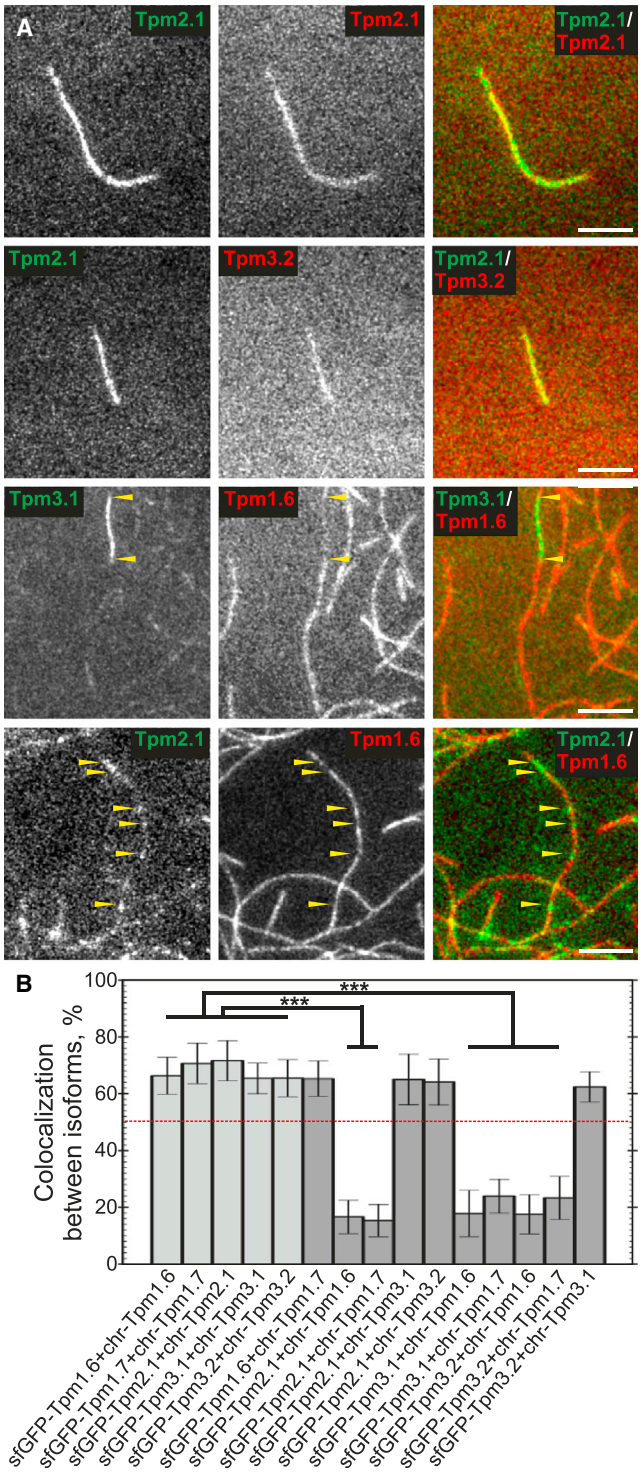

Figure 2. Co-polymerization of Tropomyosin Isoforms on F-actin Examined by an In Vitro TIRF Assay

(A) sfGFP or mCherry fusions of the tropomyosin isoforms were purified and added in pairs on 800 nM polymerizing β/γ-actin filaments, and their segregation on actin filaments was examined by total internal reflection fluorescence (TIRF) microscopy. The concentrations of sfGFP and mCherry fusions of tropomyosins were 150–360 nM and 300 nM–1.4 μM, respectively (sfGFP-Tpm1.6, 150 nM; sfGFP-Tpm1.7, 150 nM; sfGFP-Tpm2.1, 150 nM; sfGFP-Tpm3.1, 360 nM; sfGFP-Tpm3.2, 360 nM; mCherry-Tpm1.6, 300 nM; mCherry-Tpm1.7, 300 nM; mCherry-Tpm2.1, 1.4 μM; mCherry-Tpm3.1, 800 nM; mCherry-Tpm3.2, 800 nM). Examples of different tropomyosin pairs that either co-polymerize or segregate on actin filaments are shown (see also Figure S3). Yellow arrowheads indicate GFP-tropomyosin-decorated filament segments. Scale bars, 5 μm.

(B) The co-localization of the different tropomyosin isoform pairs on actin filaments was measured via the surface tool of Huygens software. The average percentage ± SD of red pixels co-localizing with green pixels (A) is shown (n = 15 filaments from three independent experiments; ***p < 0.001).

which, based on cell biological work, can associate with actin-depolymerizing factor (ADF)/cofilin on actin filaments [6]. Co-sedimentation assays and in vitro TIRF microscopy demonstrated that all stress-fiber-associated tropomyosin isoforms compete with cofilin for F-actin binding, and that the two proteins interact with filaments in a mutually exclusive manner (Figure 3A; Figure S4; data not shown). Dual-color TIRF microscopy movies also demonstrated that in most cases, mCherry-cofilin clusters grew co-operatively along actin filaments toward the pointed end, simultaneously replacing sfGFP-tropomyosin from filaments (Figure 3B; Movie S1). These data are in agreement with recent high-speed atomic force microscopy work proposing that cofilin induces a unidirectional conformational change in actin filaments toward the pointed end of the cofilin-decorated segment, thus promoting the growth of a cofilin cluster toward the filament pointed end [21]. Cofilin did not induce frequent severing of tropomyosin-decorated actin filaments in our TIRF setup because non-labeled β/γ-actin was used in our study, and severing events of bare filament segments could not be visualized. Thus, we examined the effects of tropomyosins on cofilin-mediated actin filament turnover by monitoring the decrease of pyrene-actin fluorescence resulting from filament disassembly in the presence of cofilin and vitamin D-binding protein (DBP) [22]. Interestingly, the tropomyosin isoforms tested here had very different effects on actin filament disassembly by cofilin. Tpm2.1, Tpm3.1, Tpm3.2, and Tpm4.2 were relatively inefficient in protecting actin filaments from cofilin, and only two isoforms, Tpm1.6 and Tpm1.7, efficiently protected actin filaments from cofilin-mediated disassembly (Figure 3C). This is consistent with the TIRF assays, suggesting that although all tropomyosins compete with cofilin for actin binding, Tpm1.6 and Tpm1.7 were the most efficient isoforms in competing with cofilin (Figures S4A and S4B). Similar to the non-tagged tropomyosins, also sfGFP-Tpm1.6 and sfGFP-Tpm1.7 protected actin filaments from cofilin more efficiently compared to other isoforms (Figure S4C).

Tropomyosins and an actin filament cross-linking protein, α-actinin, display typically mutually exclusive localizations in contractile actin filament structures such as myofibrils and stress fibers. However, Tpm1.6 co-localizes, at a light microscopy level, with α-actinin in the non-contractile dorsal stress fibers of migrating cells [7]. Thus, we performed actin filament co-sedimentation assays to test whether the stress-fiber-associated tropomyosins compete with non-muscle α-actinin-1 for actin filament binding in vitro. In these assays, actin filaments were pre-incubated with tropomyosins, and the ability of α-actinin to subsequently replace tropomyosins from filaments was examined. The amount of all tropomyosin isoforms on actin filaments decreased in a concentration-dependent manner after addition of α-actinin-1, suggesting that all stress-fiber-associated

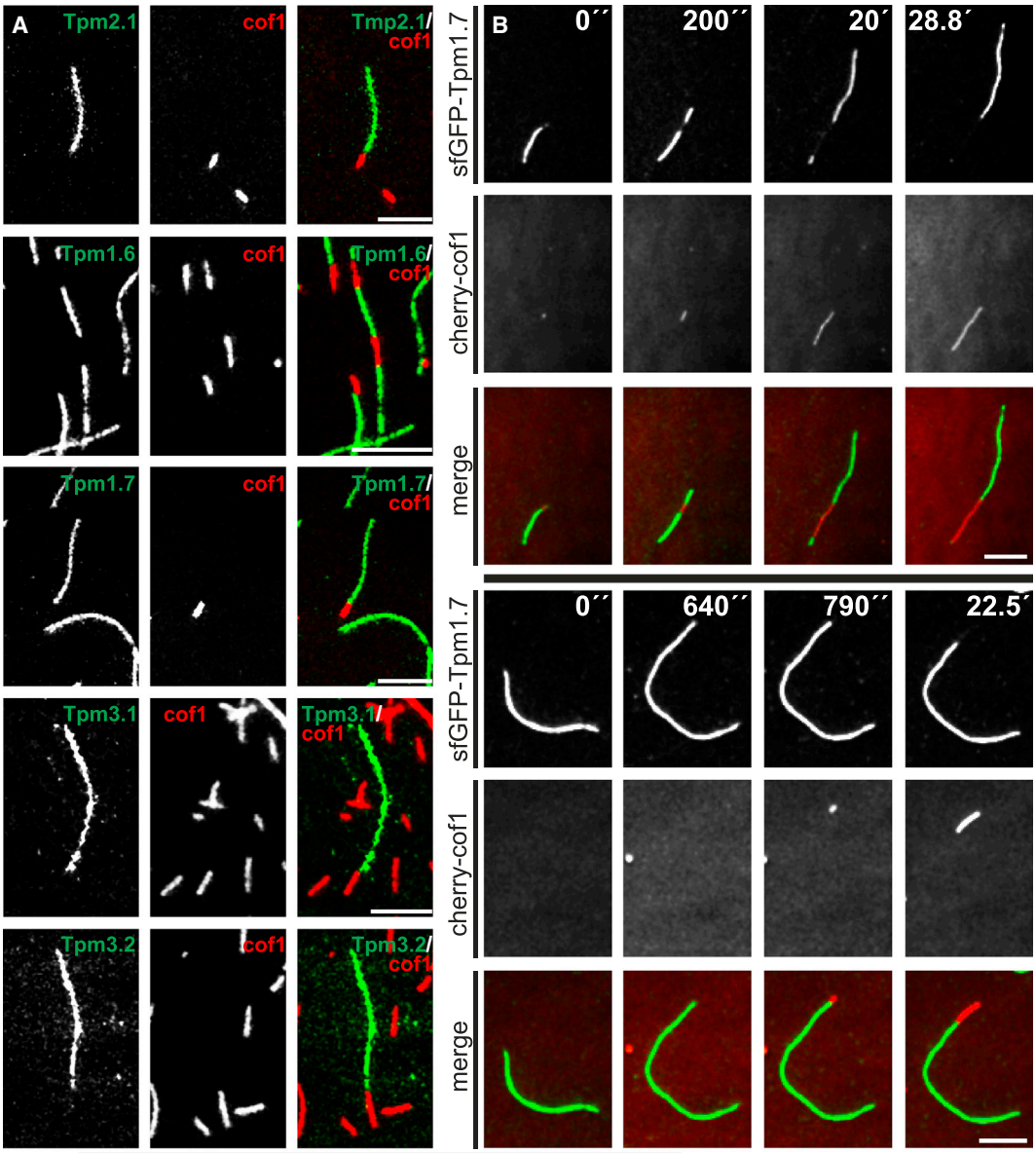

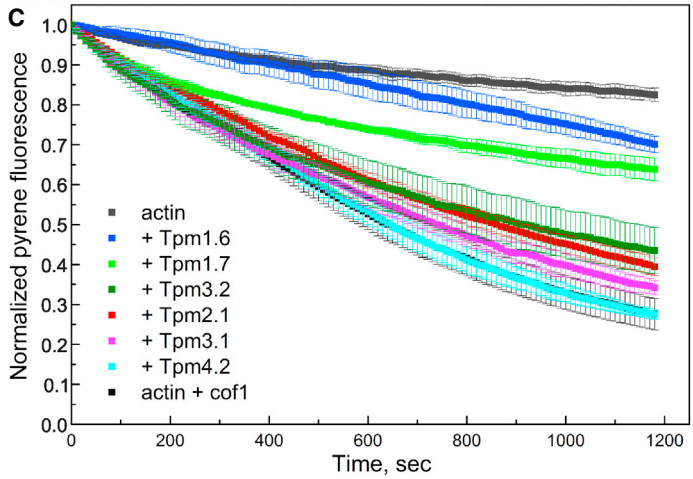

Sample	Rate	SEM
actin	0.1749	0.0044
actin+cof1	0.8003	0.0037
+Tpm 2.1	0.6343	0.0033
+Tpm 1.6	0.2795	0.0062
+Tpm 1.7	0.3385	0.0044
+Tpm 4.2	0.7591	0.0055
+Tpm 3.1	0.6791	0.0070
+Tpm 3.2	0.6065	0.0100

(legend on next page)

tropomyosin isoforms compete with α-actinin for actin filament binding (Figures 4A and 4B; Figure S4D). The order in which the proteins were added on actin filaments did not affect their competition, because similar displacement was also observed when actin filaments were first incubated with α-actinin-1 before addition of tropomyosins (data not shown). Based on cryo-electron microscopy work, the binding sites of α-actinin and tropomyosins on actin do not overlap [3, 23], and thus the molecular mechanism of competition between tropomyosins and α-actinin for actin filament binding needs to be elucidated.

Tropomyosins are well-established regulators of myosin II activity in muscle sarcomeres. Also, many non-muscle tropomyosin isoforms can affect the MgATPase activity and motility of myosins along actin filaments [24–28]. However, the effects of different stress-fiber-associated tropomyosin isoforms on myosin II have not been systematically compared. To elucidate how the decoration of actin filaments with different tropomyosin isoforms influences their interaction with myosin II, we measured the actin-activated ATPase activity of non-muscle myosin IIa heavy meromyosin (NMIIa-HMM) during steady state. These experiments revealed that whereas Tpm4.2, Tpm3.1, and Tpm3.2 efficiently increased the actin-activated ATPase activity of NMIIa-HMM, the other tropomyosin isoforms had no detectable effect on myosin IIa activity. Similar results were obtained in assays carried out with either skeletal muscle α-actin or non-muscle β-actin (Figures 4C and 4D).

Together, these experiments demonstrate that actin filaments decorated by different tropomyosin isoforms display distinct functional properties. Filaments decorated with Tpm1.6 and Tpm1.7 do not activate myosin IIa but efficiently protect filaments from cofilin-induced disassembly. On the other hand, Tpm3.1, Tpm3.2, and Tpm4.2 stimulate the actin-induced ATPase activity of myosin IIa but do not efficiently protect actin filaments from cofilin. The effects of Tpm 3.1 and Tpm4.2 on myosin IIa activity are also consistent with cell biological data providing evidence that these tropomyosin isoforms can recruit myosin II to stress fibers [6, 7]. Interestingly, the functions of tropomyosins in filament stabilization versus myosin II activation appear to correlate with the dynamics of their actin interactions. This is because Tpm1.6 and Tpm1.7 display very stable association with actin filaments, whereas Tpm3.1, Tpm3.2, and Tpm4.2 exhibit dynamic interactions with actin (Figure 4E).

Whereas other stress-fiber-associated tropomyosin isoforms either activate myosin II or protect filaments from cofilin-mediated disassembly, Tpm2.1 does not display strong effects on either of these activities. We propose that this tropomyosin isoform regulates some other aspects of stress fiber assembly, dynamics, or contractility by controlling the activity or localization of another protein(s) within the stress fiber network. Moreover, it is possible that Tpm2.1 works only in concert with some other stress fiber proteins, such as caldesmon and calponins, in cells. Interestingly, Tpm2.1 accumulates at focal adhesions at the distal ends of dorsal stress fibers, and recent studies demonstrated that it controls mechanosensitive sarcomere-like contractile units at these sites [7, 29].

In the future, it will be interesting to examine the interplay of different mammalian tropomyosin isoforms with a wider range of actin-binding proteins, including different filament cross-linkers, other myosins, the Arp2/3 complex, and profilin, which in other organisms were shown to exhibit interplay with tropomyosins on actin filaments [30–33]. Please note that, although different tropomyosin isoforms display distinct localization patterns along non-contractile dorsal stress fibers, they all localize to myosin II-containing foci in contractile ventral stress fibers. Thus, in addition to other actin-binding proteins, tropomyosins may also work in concert with each other to generate and maintain complex actin filament arrays in cells. In the context of the stress fiber network, it is possible that the non-contractile dorsal stress fibers need protection from ADF/cofilin-induced filament disassembly and are thus composed of Tpm1.6-decorated actin filaments [7]. On the other hand, actin filaments that are under myosin II-generated tension are protected from ADF/cofilins [14, 34]. These "myosin II-associating" actin filaments may not, therefore, require Tpm1.6 or Tpm1.7 to inhibit their severing by ADF/cofilins. It is also important to note that filament severing by ADF/cofilins is greatly enhanced by their co-factors, including coronin, and Aip1 in cells [35], adding more complexity to the system.

Our in vitro TIRF microscopy experiments also provide the first evidence that most tropomyosins cannot co-polymerize with each other on actin filaments but instead segregate into different filaments or filament segments. Thus, tropomyosins have the intrinsic ability to generate distinct actin filament populations that are decorated by a specific tropomyosin isoform(s), which subsequently can modulate the interactions of other proteins with these filaments. These biochemical data also provide an explanation for distinct subcellular localizations of different tropomyosin isoforms within cellular actin filament networks of motile cells [7, 36]. The molecular mechanism underlying tropomyosin isoform segregation along actin filaments remains to be elucidated. This can arise from the chemical differences of tropomyosin N and C termini that either allow or prevent end-to-end association of different tropomyosin molecules. Alternatively (or in addition), this may involve different positioning of distinct tropomyosin isoforms on actin filaments or their effects on

Figure 3. Binding of Different Tropomyosin Isoforms to Actin Filaments Modulates the Severing Activity of Cofilin-1

(A) All tropomyosin isoforms tested compete with cofilin-1 for F-actin binding. sfGFP-tagged tropomyosin isoforms (150 nM) were mixed with 150 nM mCherry-cofilin-1 on polymerizing β/γ-actin filaments, and the segregation of these two proteins on actin filaments was examined by TIRF microscopy (see also Figure S4). Scale bars, 5 μm.

(B) Examples of sfGFP-Tpm1.7 displacement by mCherry-cofilin-1 on actin filaments. sfGFP-Tpm1.7 (150 nM) was mixed with mCherry-cofilin-1 (1 μM, top; 360 nM, bottom) and polymerizing β/γ-actin, and the displacement of Tpm1.7 by cofilin-1 was observed by TIRF microscopy. Please note that in both cases the cofilin-1 cluster elongates processively toward the actin filament pointed end. Scale bars, 5 μm.

(C) Effects of different tropomyosins on the disassembly of β/γ-actin filaments. Samples of pre-polymerized pyrene β/γ-actin (4 μM) were pre-incubated for 5 min with various tropomyosins (1.25 μM) and then for 5 min with cofilin-1 (1 μM), followed by addition of the actin monomer-sequestering vitamin D-binding protein (6 μM). Data are represented as average ± SEM; n = 3–4 independent experiments. From six tropomyosins tested, only Tpm1.6 and Tpm1.7 efficiently protected actin filaments from cofilin-1-induced disassembly. The method for calculating the relative actin filament disassembly rates is described in the Supplemental Experimental Procedures.

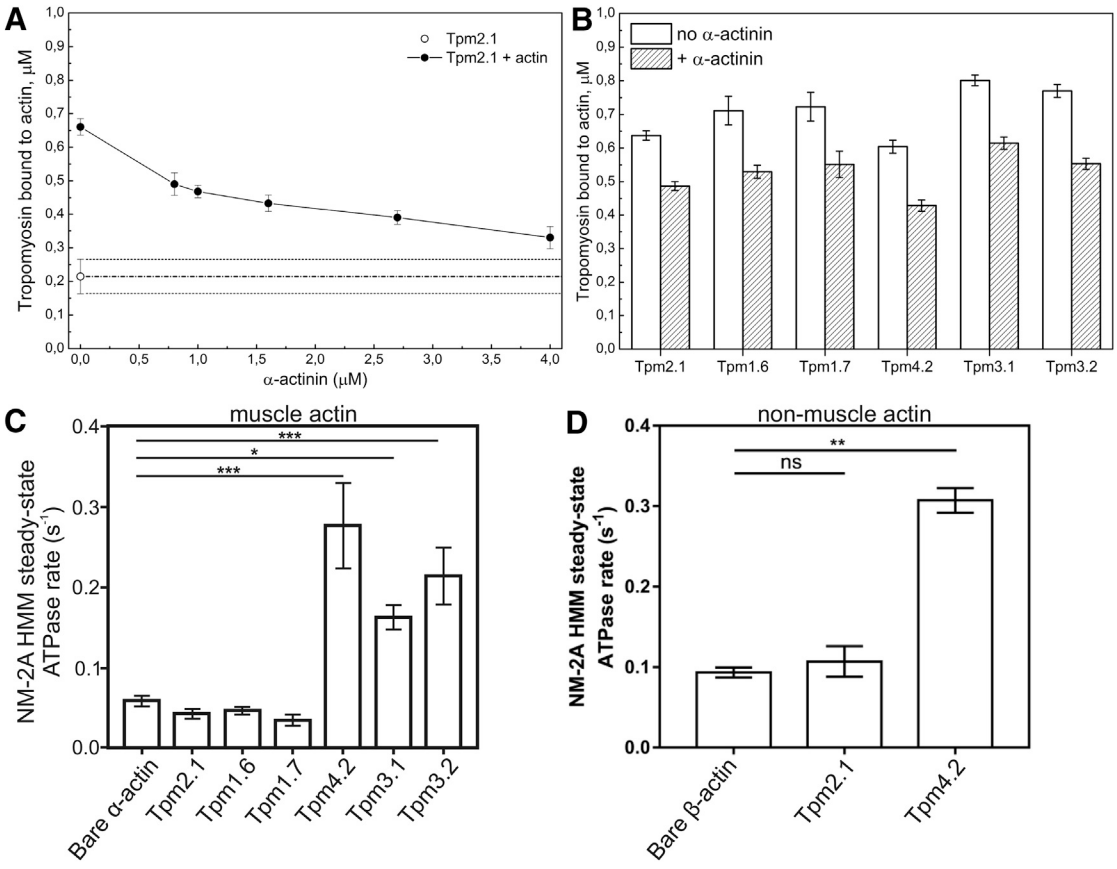

E

Tpm isoform	α-actinin competition	cofilin protection	myosin ATPase activation	dynamics
Tpm 1.6	+	+	-	slow
Tpm 1.7	+	+	-	slow
Tpm 2.1	+	-	-	slow
Tpm 3.1	+	-	+	fast
Tpm 3.2	+	-	+	fast
Tpm 4.2	+	-	+	fast

Figure 4. Effects of Tropomyosins on the Association of α-Actinin-1 and Myosin II with Actin Filaments

(A) Equilibrium binding of Tpm2.1 to β/γ-actin filaments (8 μM) in the presence of different α-actinin-1 concentrations. β/γ-actin filaments (8 μM) were pre-incubated with 0, 0.8, 1, 1.6, 2.7, and 4 μM α-actinin-1 for 30 min at room temperature, followed by incubation with Tpm2.1 (1 μM) for another 30 min. Actin filaments were sedimented via centrifugation, and the amount of tropomyosin in the pellet fractions was plotted against rising α-actinin-1 concentrations (black circles). The amount of Tpm2.1 sedimenting in the absence of actin is indicated by an open circle. Data are represented as average ± SEM; n = 3 independent experiments.

(B) β/γ-actin filaments (8 μM) were pre-incubated with different tropomyosins (1 μM) for 30 min, followed by incubation with α-actinin-1 (1.6 μM) or buffer for another 30 min. Actin filaments were sedimented, and the amounts of tropomyosins in the pellet fraction were quantified. Data are represented as average ± SEM; n = 5 independent experiments. All six tropomyosins displayed a noticeable decrease in actin-binding efficiency in the presence of α-actinin-1.

(C) The non-muscle myosin IIa-HMM steady-state ATPase rate was determined in the presence of 20 μM rabbit muscle actin and 20 μM different tropomyosin isoforms. Data were analyzed with GraphPad Prism 7 software. The Gaussian distribution of ATPase assay data was confirmed, and a one-way ANOVA was performed comparing all conditions to the bare-actin control. Data are represented as average ± SEM; n = 8–14 (*$p < 0.05$, ***$p < 0.001$).

(D) The non-muscle myosin IIa-HMM steady-state ATPase rate was determined in the presence of 20 μM β-actin and 20 μM Tpm2.1 and Tpm4.2. Similar to the experiment with rabbit muscle actin (C), Tpm2.1 did not stimulate the steady-state ATPase rate of non-muscle myosin IIa-HMM, whereas Tpm4.2 stimulated the activity of myosin IIa. Data are represented as average ± SEM; n = 6 (**$p < 0.01$; ns, not significant).

(E) A table summarizing biochemical properties of stress-fiber-associated tropomyosin isoforms.

the conformation of actin filaments. The latter alternative is supported by the fact that tropomyosins decorate the two structurally identical grooves along an actin filament, and thus their segregation cannot be solely determined by head-to-tail associations (i.e., some coordination must exist between the two tropomyosin-binding grooves when filament segments decorated by only one tropomyosin isoform exist). This may reciprocally also explain why Tpm2.1 and Tpm3.1/2, which exhibit major differences in their N-terminal sequences, do not segregate to different actin filaments in our TIRF assay.

Furthermore, the mechanisms by which different tropomyosin isoforms are targeted to their specific cellular destinations

remain to be elucidated. Good candidates for this task are formins, which at least in fission yeast can induce assembly of actin filament structures that are decorated by specific tropomyosin isoforms [37]. Intriguingly, at least four different formins are linked to the assembly of the stress fiber network in motile cells [7, 10, 11, 13], and thus these formins may provide the link between actin filament nucleation and incorporation of specific tropomyosin isoforms into the different regions of the stress fiber network.

SUPPLEMENTAL INFORMATION

Supplemental Information includes Supplemental Experimental Procedures, four figures, and one movie and can be found with this article online at http://dx.doi.org/10.1016/j.cub.2017.01.018.

AUTHOR CONTRIBUTIONS

P.L., G.G., and E.K. designed the study. P.L., A.M., P.W.G., D.J.M., E.K., and G.G. wrote the paper. G.G., E.K., T.R., T.K., K.K., L.G., and A.M. designed, performed, and analyzed the experiments. All authors approved the final manuscript.

ACKNOWLEDGMENTS

This research was supported by grants from the Academy of Finland Center of Excellence Program (272130), Sigrid Juselius Foundation, and Jane and Aatos Erkko Foundation (to P.L.), NHMRC (APP1004188) and Kids Cancer Network (to P.W.G.), Deutsche Forschungsgemeinschaft (MA 1081/22-1; to D.J.M.), and Ella and Georg Ehrnrooth Foundation (to E.K.). A.M. was supported by the ERC (SegregActin no. 638376) and Labex INFORM (ANR-11-LABX-0054; funded by the Investissements d'Avenir French Government Program). We acknowledge the France-BioImaging infrastructure supported by the French National Research Agency (ANR-10-INSB-04-01). Aleksi Ainonen, Markus Korpela, and Anna-Liisa Nyfors are acknowledged for technical support. We thank Mikko Liljeström and the Biomedicum Imaging Unit for excellent technical support with microscope equipment and in vitro TIRF data analysis. Kristina Djinovic-Carugo (Vienna) is acknowledged for providing the α-actinin-1 expression vector. P.W.G. is a non-executive director of Novogen, a company that is commercializing anti-tropomyosin drugs for the treatment of cancer.

Received: August 30, 2016
Revised: December 14, 2016
Accepted: January 10, 2017
Published: February 16, 2017

REFERENCES

1. Michelot, A., and Drubin, D.G. (2011). Building distinct actin filament networks in a common cytoplasm. Curr. Biol. *21*, R560–R569.
2. Gunning, P.W., Hardeman, E.C., Lappalainen, P., and Mulvihill, D.P. (2015). Tropomyosin - master regulator of actin filament function in the cytoskeleton. J. Cell Sci. *128*, 2965–2974.
3. von der Ecken, J., Müller, M., Lehman, W., Manstein, D.J., Penczek, P.A., and Raunser, S. (2015). Structure of the F-actin-tropomyosin complex. Nature *519*, 114–117.
4. Manstein, D.J., and Mulvihill, D.P. (2016). Tropomyosin-mediated regulation of cytoplasmic myosins. Traffic *17*, 872–877.
5. Ono, S., and Ono, K. (2002). Tropomyosin inhibits ADF/cofilin-dependent actin filament dynamics. J. Cell Biol. *156*, 1065–1076.
6. Bryce, N.S., Schevzov, G., Ferguson, V., Percival, J.M., Lin, J.J., Matsumura, F., Bamburg, J.R., Jeffrey, P.L., Hardeman, E.C., Gunning, P., and Weinberger, R.P. (2003). Specification of actin filament function and molecular composition by tropomyosin isoforms. Mol. Biol. Cell *14*, 1002–1016.
7. Tojkander, S., Gateva, G., Schevzov, G., Hotulainen, P., Naumanen, P., Martin, C., Gunning, P.W., and Lappalainen, P. (2011). A molecular pathway for myosin II recruitment to stress fibers. Curr. Biol. *21*, 539–550.
8. Gunning, P.W., Ghoshdastider, U., Whitaker, S., Popp, D., and Robinson, R.C. (2015). The evolution of compositionally and functionally distinct actin filaments. J. Cell Sci. *128*, 2009–2019.
9. Tojkander, S., Gateva, G., and Lappalainen, P. (2012). Actin stress fibers–assembly, dynamics and biological roles. J. Cell Sci. *125*, 1855–1864.
10. Hotulainen, P., and Lappalainen, P. (2006). Stress fibers are generated by two distinct actin assembly mechanisms in motile cells. J. Cell Biol. *173*, 383–394.
11. Ang, S.F., Zhao, Z.S., Lim, L., and Manser, E. (2010). DAAM1 is a formin required for centrosome re-orientation during cell migration. PLoS ONE *5*, e13064.
12. Gateva, G., Tojkander, S., Koho, S., Carpen, O., and Lappalainen, P. (2014). Palladin promotes assembly of non-contractile dorsal stress fibers through VASP recruitment. J. Cell Sci. *127*, 1887–1898.
13. Skau, C.T., Plotnikov, S.V., Doyle, A.D., and Waterman, C.M. (2015). Inverted formin 2 in focal adhesions promotes dorsal stress fiber and fibrillar adhesion formation to drive extracellular matrix assembly. Proc. Natl. Acad. Sci. USA *112*, E2447–E2456.
14. Tojkander, S., Gateva, G., Husain, A., Krishnan, R., and Lappalainen, P. (2015). Generation of contractile actomyosin bundles depends on mechanosensitive actin filament assembly and disassembly. eLife *4*, e06126.
15. Monteiro, P.B., Lataro, R.C., Ferro, J.A., and Reinach, Fde.C. (1994). Functional alpha-tropomyosin produced in *Escherichia coli*. A dipeptide extension can substitute the amino-terminal acetyl group. J. Biol. Chem. *269*, 10461–10466.
16. Brooker, H.R., Geeves, M.A., and Mulvihill, D.P. (2016). Analysis of biophysical and functional consequences of tropomyosin-fluorescent protein fusions. FEBS Lett. *590*, 3111–3121.
17. Janco, M., Bonello, T.T., Byun, A., Coster, A.C., Lebhar, H., Dedova, I., Gunning, P.W., and Böcking, T. (2016). The impact of tropomyosins on actin filament assembly is isoform specific. BioArchitecture *6*, 61–75.
18. Nishida, E., Maekawa, S., and Sakai, H. (1984). Cofilin, a protein in porcine brain that binds to actin filaments and inhibits their interactions with myosin and tropomyosin. Biochemistry *23*, 5307–5313.
19. Bernstein, B.W., and Bamburg, J.R. (1982). Tropomyosin binding to F-actin protects the F-actin from disassembly by brain actin-depolymerizing factor (ADF). Cell Motil. *2*, 1–8.
20. Robaszkiewicz, K., Ostrowska, Z., Marchlewicz, K., and Moraczewska, J. (2016). Tropomyosin isoforms differentially modulate the regulation of actin filament polymerization and depolymerization by cofilins. FEBS J. *283*, 723–737.
21. Ngo, K.X., Kodera, N., Katayama, E., Ando, T., and Uyeda, T.Q. (2015). Cofilin-induced unidirectional cooperative conformational changes in actin filaments revealed by high-speed atomic force microscopy. eLife *4*, e04806.
22. Gandhi, M., Achard, V., Blanchoin, L., and Goode, B.L. (2009). Coronin switches roles in actin disassembly depending on the nucleotide state of actin. Mol. Cell *34*, 364–374.
23. Galkin, V.E., Orlova, A., Salmazo, A., Djinovic-Carugo, K., and Egelman, E.H. (2010). Opening of tandem calponin homology domains regulates their affinity for F-actin. Nat. Struct. Mol. Biol. *17*, 614–616.
24. Hodges, A.R., Krementsova, E.B., Bookwalter, C.S., Fagnant, P.M., Sladewski, T.E., and Trybus, K.M. (2012). Tropomyosin is essential for processive movement of a class V myosin from budding yeast. Curr. Biol. *22*, 1410–1416.
25. Barua, B., Nagy, A., Sellers, J.R., and Hitchcock-DeGregori, S.E. (2014). Regulation of nonmuscle myosin II by tropomyosin. Biochemistry *53*, 4015–4024.

26. Clayton, J.E., Pollard, L.W., Murray, G.G., and Lord, M. (2015). Myosin motor isoforms direct specification of actomyosin function by tropomyosins. Cytoskeleton *72*, 131–145.
27. Hundt, N., Steffen, W., Pathan-Chhatbar, S., Taft, M.H., and Manstein, D.J. (2016). Load-dependent modulation of non-muscle myosin-2A function by tropomyosin 4.2. Sci. Rep. *6*, 20554.
28. Sckolnick, M., Krementsova, E.B., Warshaw, D.M., and Trybus, K.M. (2016). Tropomyosin isoforms bias actin track selection by vertebrate myosin Va. Mol. Biol. Cell *27*, 2889–2897.
29. Wolfenson, H., Meacci, G., Liu, S., Stachowiak, M.R., Iskratsch, T., Ghassemi, S., Roca-Cusachs, P., O'Shaughnessy, B., Hone, J., and Sheetz, M.P. (2016). Tropomyosin controls sarcomere-like contractions for rigidity sensing and suppressing growth on soft matrices. Nat. Cell Biol. *18*, 33–42.
30. Skau, C.T., and Kovar, D.R. (2010). Fimbrin and tropomyosin competition regulates endocytosis and cytokinesis kinetics in fission yeast. Curr. Biol. *20*, 1415–1422.
31. Clayton, J.E., Sammons, M.R., Stark, B.C., Hodges, A.R., and Lord, M. (2010). Differential regulation of unconventional fission yeast myosins via the actin track. Curr. Biol. *20*, 1423–1431.
32. Hsiao, J.Y., Goins, L.M., Petek, N.A., and Mullins, R.D. (2015). Arp2/3 complex and cofilin modulate binding of tropomyosin to branched actin networks. Curr. Biol. *25*, 1573–1582.
33. Alioto, S.L., Garabedian, M.V., Bellavance, D.R., and Goode, B.L. (2016). Tropomyosin and profilin cooperate to promote formin-mediated actin nucleation and drive yeast actin cable assembly. Curr. Biol. *26*, 3230–3237.
34. Hayakawa, K., Tatsumi, H., and Sokabe, M. (2011). Actin filaments function as a tension sensor by tension-dependent binding of cofilin to the filament. J. Cell Biol. *195*, 721–727.
35. Jansen, S., Collins, A., Chin, S.M., Ydenberg, C.A., Gelles, J., and Goode, B.L. (2015). Single-molecule imaging of a three-component ordered actin disassembly mechanism. Nat. Commun. *6*, 7202.
36. Brayford, S., Bryce, N.S., Schevzov, G., Haynes, E.M., Bear, J.E., Hardeman, E.C., and Gunning, P.W. (2016). Tropomyosin promotes lamellipodial persistence by collaborating with Arp2/3 at the leading edge. Curr. Biol. *26*, 1312–1318.
37. Johnson, M., East, D.A., and Mulvihill, D.P. (2014). Formins determine the functional properties of actin filaments in yeast. Curr. Biol. *24*, 1525–1530.